Design and Testing of Iowa State University's AABL Wind and Gust Tunnel

by

Partha P. Sarkar[1] and Fred L. Haan, Jr.[2]

ABSTRACT

A wind tunnel with advanced capabilities will aid research efforts to understand the complex fluid structure interaction problems encountered in wind engineering since wind tunnels remain an integral component of the design process for wind sensitive structures. Whether dealing with the aerodynamics of buildings, bridges or towers many issues remain to be fully resolved—including the role of non-stationary gust interactions, Reynolds number effects, and the significance of small-scale turbulence. Building the next generation of such wind tunnels will contribute to the understanding of these issues and create the research infrastructure necessary to meet the challenges of wind hazards in the USA and elsewhere.

A combination Aerodynamic/Atmospheric Boundary Layer (AABL) Wind and Gust Tunnel with a unique active gust generation capability has been developed for wind engineering and industrial aerodynamics applications. The AABL Wind and Gust Tunnel is primarily a closed-circuit tunnel that can be also operated in open-return mode. It is designed to accommodate two test sections (2.44m x 1.83m and 2.44m x 2.21m) with a maximum wind speed capability of 53 m/s. The gust generator is capable of producing non-stationary gust magnitudes around 27% of the mean flow speed. This paper describes the motivation for developing this advanced wind tunnel and the work related to its design and testing.

KEYWORDS: wind tunnel, active gust generation, non-stationary flow, wind engineering, industrial aerodynamics

1.0 INTRODUCTION

Building wind tunnels with advanced capabilities will aid research efforts to understand the complex fluid structure interaction problems encountered in wind engineering design. Computer simulations currently are inadequate for design of bluff bodies because of the complexity of the fluid dynamics involved. Wind tunnels remain an integral component of the design process for wind sensitive structures.

Boundary layer wind tunnels have played an integral role in the design of wind-sensitive structures for decades. Capable of simulating the lower portion of the earth's atmospheric boundary layer, these tunnels have enabled the safe design of long-span bridges, tall buildings, towers, and a host of other unique structures. With regard to the aerodynamics of these structures, many issues remain to be fully resolved—including the role of non-stationary gust interactions, Reynolds number effects, and the significance of small-scale turbulence. Research into these issues is currently limited by the capabilities of existing wind tunnels.

A combination Aerodynamic/Atmospheric Boundary Layer (AABL) Wind and Gust Tunnel with a unique active gust generation capability has been developed for *wind engineering* and

1 Professor and Wilson Chair, 2 Assistant Professor
Wind Simulation and Testing Laboratory, Department of Aerospace Engineering, Iowa State University, 2271 Howe Hall, Room 1200, Ames, IA 50011-2271 USA

industrial aerodynamics applications. The AABL Wind and Gust Tunnel is primarily a closed-circuit tunnel that can be also operated in open-return mode. It is designed to accommodate two test sections (2.44m x 1.83m and 2.44m x 2.21m) with a maximum wind speed capability of 53 m/s. The gust generator is capable of producing non-stationary gust magnitudes around 27% of the mean flow speed. This wind tunnel is one of the several wind tunnels that are housed in the Wind Simulation and Testing Laboratory (WiST Lab) in the Department of Aerospace Engineering at Iowa State University. This paper describes the motivation for developing this advanced wind tunnel and the work related to its design and testing.

The motivation for a tunnel with advanced gusting features arose from the primary assumption in the current practice of boundary layer wind tunnel testing—that atmospheric velocity variations can be adequately modeled by stationary mean and turbulent flow properties. Extreme wind loads, however, result primarily from extreme weather events (such as gust fronts, hurricanes, etc.) where non-stationary gusts, transitional flow structures and rapid wind directionality changes may play a significant role. The current state-of-the-art boundary layer wind tunnels are incapable of physically simulating the transient effects of such events. Building the next generation of such wind tunnels will contribute to the research infrastructure necessary to meet the challenges of wind hazards in this country. Better simulations of atmospheric flows will enhance our understanding of the various fluid structure interaction phenomena involved and greatly enhance our ability to develop mitigation measures.

Understanding how the construction of wind tunnels with advanced capabilities constitutes a worthy endeavor requires some background into the use of wind tunnels in wind engineering and into the technical problems faced by wind engineers. This section provides such background by providing a general introduction to atmospheric boundary layer (ABL) wind tunnels—the wind engineer's tool of choice for the past several decades.

2.0 BACKGROUND

2.1 Boundary-Layer Wind Tunnel

Wind tunnel simulation of the earth's atmospheric boundary layer is a well-established practice. Numerous researchers have contributed to the set of tools now in use for generating wind tunnel boundary layers that are several feet deep (for example, Cermak, 1971; Cook, 1973; Davenport, 1966; Farell and Iyengar, 1999). Conventional approaches employ a combination of passive devices such as spires, barrier walls, and floor roughness to generate boundary layers of the same scale as the geometric scaling of structural models placed in them. These models are then tested in a statistically stationary flow environment where the wind tunnel velocity profile, turbulence intensity profile, integral length scales and velocity spectra are matched to the scaled field values.

It is assumed that atmospheric velocity variations can be adequately modeled by stationary mean and turbulent flow properties. This assumption means that despite the fact that hurricanes and gust fronts can have non-stationary characteristics, wind sensitive structures are tested in stationary flow environments. Wind tunnel turbulence intensities are matched to site values, and wind tunnel integral scales are scaled with the geometric scale of the structural models. While this conventional approach has served (and still serves) research and industrial needs for some time, the following two sections summarize how new tunnel capabilities can answer questions that cannot be addressed with the current generation of wind tunnels.

2.2 Turbulence Effects

The role of turbulence in the relevant fluid-structure interaction problems will influence the wind tunnel design. While some of the characteristics of atmospheric turbulence have been simulated sufficiently well for some time (for example, boundary layer velocity profiles, scaling of turbulence integral scales with model dimensions, etc.) other turbulence characteristics cannot be simulated precisely at all or cannot be simulated without considerable effort. This section briefly describes the role that turbulence plays in wind engineering and how new capabilities in wind tunnels can improve our understanding of these complex fluid-structure interaction problems.

Civil engineering structures do not, in general, have aerodynamic performance as their primary design goal. As a result, most civil engineering structures can be classified as bluff rather than streamlined bodies. Bluff bodies experience flow separation over significant portions of their surface. Bluff body aerodynamics differs from aerodynamics of streamlined bodies in that flow separation and reattachment play primary roles in pressure distributions about bodies of interest.

Free stream turbulence can modify the behavior of shear layers separating from bluff bodies. These modifications lead to flow structure changes and pressure distribution changes.

The role of turbulence in the aerodynamics of bluff bodies has been extensively documented in the literature (e.g., Gartshore, 1973; Kareem & Cermak, 1979; Hillier & Cherry, 1981; Bearman & Morel, 1983; Nakamura & Ohya, 1984; Kiya & Sasaki, 1985; Saathoff & Melbourne, 1997; and others). What is clear is that turbulence scales influence aerodynamic properties (such as rms and peak pressure coefficients). What is not clear is the extent of these influences.

When considering the smallest scales of turbulent velocity fluctuations, the inertial subrange is a relevant concept. The "inertial subrange" of a turbulent flow refers to that range of turbulent eddy scales between the large inviscid energy-containing scales and the small viscous diffusion scales. The size of the small, energy dissipating scales decreases with increasing Reynolds number—which accompanies an increase in the size of the inertial subrange. The size of the inertial subrange is relevant to bluff body aerodynamics because the size of the subrange impacts the amount of turbulent energy residing at small scales. Small scale content—particularly scales on the order of the thickness of the separated shear layer—has been shown by a number of researchers to have a significant effect on separated shear layer flow structure (Gartshore, 1973; Tieleman & Akins, 1990).

A significant difference in small-scale turbulence content can exist between wind tunnel and full-scale flows because wind tunnel Reynolds numbers can be as much as three orders of magnitude lower than those of atmospheric flows. To quantify small-scale content, a "small-scale spectral density parameter" was originally suggested by Melbourne (1979) and subsequently used by Tieleman and Akins (1990). This parameter is essentially a *scale-specific* turbulence intensity. Tieleman and Akins reported that wind tunnel simulations with insufficient small scale content resulted in poorer comparisons of pressure coefficients between model and full-scale results.

The above may not fully address all issues relating to Reynolds number mismatches. Rather, it illustrates one of the ramifications of failing to match Reynolds numbers in wind tunnel simulations. Decreasing Reynolds number disparities between model and prototype flows will increase our confidence in test results. Understanding the physics of *how* flows depend on Reynolds number will decrease the uncertainty associated with imperfect turbulence simulation. Wind tunnels capable of higher Reynolds numbers would enable study of such questions.

2.3 Non-Stationary Flow Simulation

In addition to Reynolds number and small-scale turbulence issues, large-scale turbulent gusts also constitute an important aspect of wind tunnel simulation. Passive turbulence generation techniques (such as the obstacles described previously) have been shown to produce only a limited range of possible integral scales (Bienkiewicz et al., 1983). These scales are often not large enough to match prototype scales. As a result, active turbulence generation schemes have been developed to produce integral scales up to an order of magnitude larger than those of passive techniques. These techniques generally involve grids, flaps, airfoils (and combinations of them) that are forced to oscillate (Bienkiewicz et al., 1983; Kobayashi et al., 1994; Cermak et al., 1995).

While such devices are useful for generating stationary velocity fluctuations, they have not generally been used to simulate the non-stationary gusts that can occur in hurricanes and thunderstorms. Anemometry data from hurricanes has shown that velocity records are non-stationary at times (Schroeder & Smith, 1999). Thus far, however, no wind tunnel studies have investigated the impact of such non-stationarity on aerodynamic pressures on structures. While advanced analytical simulation methods for non-stationary wind fluctuations are being developed (Chen and Letchford, 2005; Wang and Kareem, 2005), little experimental work in this area has been attempted. The next generation of ABL wind tunnel should have the capability to conduct such tests.

In addition to simulating large-scale gusts, wind direction changes can be simulated with active turbulence generation equipment. Wind direction changes have been observed to significantly affect pressure distributions on building models in wind tunnels (Wu et al., 2001a; Wu et al., 2001b). Next generation ABL wind tunnels will also be used for furthering research of this type.

3. DESIGN OF THE WIND TUNNEL

This section describes the various components of the Aerodynamic/Atmospheric Boundary Layer (AABL) Wind and Gust Tunnel and discusses their performance. The conception and design of the wind tunnel began in August 2000 and was completed in February 2003. The construction of the wind tunnel began in November 2003 and was completed in October 2005. The design objectives were set on the basis of research needs and two main considerations which were minimizing the cost of construction and accommodating the wind tunnel within the available building space. It was desired to have two test sections, one for uniform flow with low turbulence and the other for atmospheric boundary layer flow with moderate to high turbulence, with a gust generation capability.

The design included non-stationary flow capability, a reasonably high-speed capacity and a large cross-section to accommodate realistic models. The wind tunnel was conceived as a closed-circuit type with the option of running it in an open-circuit mode. The dimensions were fixed as 2.44 m (8 ft) wide by 1.83 m (6 ft) high for the Aero (aerodynamic) test section followed by 2.44 m (8 ft) wide by 2.21 m (7.25 ft) high ABL test section to simulate atmospheric boundary layer wind. The maximum desirable speed in the Aero test section was 47.8 m/s (107 mph) and the maximum desirable speed in the ABL test section was 40 m/s (90 mph). High velocity capability combined with a relatively large test section would allow larger Reynolds numbers—with the accompanying increase in small-scale turbulent spectral content. A large working cross section would accommodate both large-scale models and large-scale velocity structures.

3.1 Component Description

Details of various components including the test sections, plenum, contraction, turning sections, heat exchanger, diffusers, and fan are given below and shown in Figure 1.

3.1.1 Fan and Motor

The fan is a Howden-Buffalo 108-50-710 model with 2.74m (9 ft or 108 in.) tip-to-tip blade diameter, 1.27m (4.2 ft or 50 in.) hub diameter with a specific flow rate of 214 m^3/s (452,000 cfm) generated at a static pressure of 870 Pa (3.5 in. water) and rotating speed of 710 rpm. The fan is driven by a 260 kW (350 hp) 3-phase, 460 volts AC motor.

3.1.2 By-Pass Duct

The By-Pass Duct is the most innovative portion of the AABL Wind and Gust Tunnel. In most wind tunnels, air speeds can be changed by increasing the speed of the fan, which causes a relatively slow change in test section velocities. However, the By-Pass Duct allows the wind and gust tunnel to change the test section velocity almost instantaneously - creating wind gust which more accurately represents the natural wind. This type of unsteady flow simulation is extremely important and opens up a new world of testing opportunities for research in unsteady-flow aerodynamics. This component is described in detail later.

3.1.3 Diffusers

There are three diffusers in this wind tunnel. These diffusers are located downstream of the test sections where maximum speed is generated. The function of a diffuser is to slow down the flow speed so that the pressure loss is minimized. The flow speed decreases as a result of gradual increase in the area of cross section of a diffuser along its length that is obtained by providing inclination angles to the side walls and/or the ceiling and floor. The first of the three diffusers is a two-dimensional plane-walled diffuser with constant width (area ratio is 1.10) and inclined ceiling that connects the ABL test section to the first corner, where its ceiling increases from 2.21m (7.25 ft) to 2.44m (8.00 ft) in 2.29 m (7.5 ft) length. The second diffuser is a three-dimensional plane-walled diffuser with area ratio of 3.5 and overall length of 19.1m (62.5 ft). It connects the 2.68m (8.80 ft) wide x 2.44m (8.02 ft) high rectangular end of the transition (first component) to a 5.03m (16.5 ft) wide x 4.1m (13.5 ft) high cross section before the heat exchanger and the third turn. The third diffuser is two-dimensional plane-walled diffuser with constant width and area ratio of 1.03. It connects 5.03m (16.5 ft) wide by 4.1 m (13.5 ft) high section at the exit of the third corner to 5.18m (17 ft) wide by 4.1m (13.5 ft) high section at the entry of the fourth corner over a length of 2.06m (6.75 ft). There is a constant section between the third diffuser and the fourth corner to accommodate a screen that will be used only if it is required. This section is 0.152m (0.5 ft) in length.

3.1.4 Heat Exchanger

The heat exchanger makes it possible to maintain a constant temperature inside the wind tunnel. Heat released by the fan and motor would cause the temperature inside a closed-circuit tunnel to continuously rise – leading to inaccuracies in experiments. The heat exchanger operates in a similar fashion as a radiator of a car, except that in this case the “radiator” is absorbing heat from the air instead of releasing it into the air, i.e. it functions as a heat sink. It is essentially made of a coil to which numerous fins are attached. Chilled water is run through the coil to remove the unwanted heat produced by the fan and motor. This heat exchanger requires 80 gpm (gallons per minute) of chilled water at 45°F to remove 9,200 BTU/min. of heat produced in the wind tunnel at 85% of the design flow capacity to maintain a constant temperature of 75 deg. F. Six coils were used with two side-by-side units of three coils stacked one above another in a staggered configuration to reduce blockage area.

3.1.5 Turning Vanes

Turning vanes help to change the direction of the air flow as it goes through a corner by directing it in the proper direction. There are 34 vanes (curved pieces of sheet metal) at each of the first two corners, as shown (Figure 1h), and 70 and 72 vanes, respectively, at the third and fourth corners. The benefits of using turning vanes include: retaining the velocity profile as the flow turns at the corner and minimizing the pressure loss at the corner.

3.1.6 Plenum

The plenum section (17 feet wide by 13.5 feet high) of the wind tunnel precedes the contraction, and its main purpose is to reduce the turbulence and increase the uniformity in the flow. This section consists of three screens (Mesh10 or M10) with spacing between the screens to reduce turbulence and a honeycomb that acts as a “flow straightener.” The porosity or open area ratio of the screens is 64%. It is planned to add up to two additional screens, if necessary. The aluminum honeycomb (HEXCEL) has hexagonal cells, 12.7mm (0.5 inch) in cell size and 20.3cm (8 inches) in length.

3.1.7 Contraction

The contraction is that section of the wind tunnel in which the cross section is greatly reduced to speed up the flow and make the flow more uniform. The mass of air per unit time that flows through the large end of the contraction must exit out of the smaller end of the contraction (principle of conservation of mass). The only way this can happen is if the air speeds up as the cross sectional area is reduced. The result is that the air moving in the test section is moving much faster than the air in the sections before contraction. The contraction ratio (ratio of the inlet area to the exit area of the contraction) is 4.78 that means the flow speeds up from 10 m/s or 22.4 mph to 47.8 m/s or 107 mph before it exits the contraction at full speed. The length of the contraction, L_c, is 5.94m (19.5 ft). Two cubic shaped profiles with matching point at a distance of $0.45L_c$ from the inlet of the contraction were used for each of the four walls.

3.1.8 Test Sections

The AABL Wind and Gust Tunnel's test section is different from most wind tunnels because the section allows for two types of testing. The first portion of the test section, 2.44m (8 ft) wide by 1.83m (6 ft) high (*Aero* test section) that immediately follows the contraction is for testing aerodynamic models. Typical aerodynamic models would be airplanes, wings of airplanes, cars, etc., that often require minimum turbulence and high speed for testing. The second portion of the wind tunnel, 2.44m (8 ft) wide by 2.21m (7.25 ft) high (*ABL* test section), is devoted to atmospheric boundary layer simulation. Buildings, bridges, and other structures encounter a more turbulent flow than airplanes. It also requires the mean velocity to increase and turbulence levels to decrease with height. The ceiling of the test section is adjustable, to allow the boundary layer growth without accelerating the flow.

3.1.9 Closed and Open-Return Modes

Most wind tunnels are either Open Return – which means air is taken in at one end and expelled from the other - or Closed Return – which means the air circulates inside the wind tunnel in a loop. Both open- and closed- return tunnels have pros and cons and that is why the AABL Wind and Gust tunnel is designed to work both as an open- and a closed-return tunnel.

The facility’s open-return mode is configured by eliminating the sets of turning vanes at the two successive corners that follow the test sections. Both sets of turning vanes have wheels at their base to allow them to be moved into the 4.9m (16 ft) duct that connects these corners. This duct is then isolated from the rest of the wind tunnel by two hinged doors, one at each corner. Each door forms part of one side of the corner section which becomes its perpendicular side once rotated, thereby opening the corner section to the outside and forming a U-shaped wind tunnel flow circuit.

3.2 Active Gust Generation using a By-Pass Duct Configuration

It has been stated previously that a number of different methods of turbulence generation have been implemented by other researchers. To create the flow features, as specified in the objectives of this work, conventional means like the oscillating vanes or airfoils used in the past by others would not be practical. Changing the mean flow speed using “lossy” devices such as vanes requires the fan to operate well off of optimal conditions and induces sudden changes in electrical power requirements. Flow speed changes could also be accomplished by changing the speed of the fan—but the inertia of the fan precludes speed changes on time scales required (25% test section speed change in 1-5 sec).

The basic design that was chosen to achieve the requirements was a bypass duct. The bypass duct (conceptually similar to the transition facility described in Saric, 1992) diverts flow from the main duct. This diversion reduces the flow velocity in the main test section. Computer-controlled dampers dictate the amount of flow diverted and the time scales involved. Several configurations of ducting were tested using small scale physical models. Hot wire probes were used to obtain velocity profiles to determine how uniformly air could be diverted from the main duct. The final concept can be seen in the wind tunnel layout diagram shown in Figures 1 and 2.

Several issues guided the design of the bypass duct. First, the amount of flow diverted through the duct had to result in a reasonable amount of velocity change in the main test section. Two rectangular ducts 4.12m (13.5 ft) high by 0.46m (1.5 ft) wide were designed for the bypass ducts. The size of these ducts was rather seriously constrained by the building geometry. They were designed to be as large as possible given the room size. These ducts run parallel to the main duct just outside the fan and represent a bypass area of 84% of the main test section's area. Second, the bypass duct and its accompanying transition sections must minimize the amount of flow non-uniformity introduced into the main duct of the wind tunnel. This issue had two major ramifications. Removing air from the stream downstream of the fan—and upstream of the test section—may introduce large non-uniformities in the mean flow profile at the test sections that would adversely affect testing. Also, reintroducing air just upstream of the fan could inject non-uniform profiles into the fan and subject the fan to damaging unsteady periodic loading.

To address these issues—and to accommodate the building geometry—the duct transition sections were designed to take air out of and put air into the main duct evenly around its entire perimeter. The two sections of the main duct on each side of the fan have circular cross sections, so this was accomplished using a 0.61m (2 ft.) wide slot along the circumference of each of these sections. Surrounding each slot is a large plenum that acts as a transition from the slot to the bypass ducts. The plenum allows the flow to reorganize from the slot to the bypass duct. These slots can be completely covered to allow the wind tunnel to operate like a regular wind tunnel—as if the bypass ducts do not exist. They are only open when the gusting capability is required.

Each bypass duct is designed with a set of electromechanically controlled dampers to open and close the duct. They consist of Ruskin heavy duty, opposed-blade airfoil dampers. Each duct has 20 blades in a 46 cm by 411 cm (18 in. by 162 in.) configuration. The dampers can be fully open, fully closed, or fixed partially open. The damper system also has a dynamic response capability for more complex gust simulations.

3.1.1 Gust Magnitude Predictions

To predict the performance of the bypass duct concept, a set of analytical tools was derived. A small scale prototype system to test the bypass duct concept was also designed and built. By validating the analytical predictions with the results of the prototype tests, reasonable performance estimates for the full scale system were obtained. This section briefly describes the analytical tools that were developed to test them.

To predict the magnitude of the gusts that could be generated with this system, estimates had to be made of the difference in wind tunnel *Aero* test section velocity, V_{WT}, when the bypass duct was open or closed. Wind tunnel velocities (again, in the *Aero* test section) for the bypass duct open and closed are denoted here as V_{WTopen} and $V_{WTclosed}$, respectively.

To estimate the test section velocity when the bypass duct is closed, one must estimate the pressure drop through the entire tunnel circuit and use the fan curve to estimate total flow rate. To estimate the pressure drop, loss coefficients were calculated for each element of the wind tunnel—diffusers, ducts, turns, screens, etc. These loss coefficients were summed into an overall loss coefficient for the wind tunnel. This loss coefficient was then related to the pressure drop through the tunnel as:

$$\Delta p_{WTclosed} = \frac{1}{2}\rho V_{WTclosed}^{2} K_{L}^{WT_{closed}} \qquad (1)$$

where $\Delta p_{WTclosed}$ is the total pressure drop of the main circuit when the bypass ducts are closed and

$K_L^{WT_{closed}}$ is the loss coefficient (referenced to the *Aero* test section velocity) of the main circuit when the bypass duct is closed. One issue should be noted here. The loss coefficient, K_L^{WT}, will have three different values depending on the configuration of the wind tunnel for each mode of operation (closed or open return). When the exit and entry slots of the bypass duct are covered, you have one loss coefficient denoted $K_L^{WT_{clean}}$. The design velocity, design static pressures and loss coefficients (with respect to Aero test section), as estimated for each component of the wind tunnel with these slots closed, is given in Table 1 where $K_L^{WT_{clean}}$ was estimated as 0.64. When the slots are open, then the loss coefficients are denoted as $K_L^{WT_{open}}$ and $K_L^{WT_{closed}}$ corresponding to the bypass duct dampers being open and closed, respectively. Values for each coefficient are listed in Table 2 (all for the wind tunnel in closed-return mode). K_L^{BD} was estimated by modeling the bypass duct as a series of individual components such as dividing flows, area contractions, etc. The details of these calculations are beyond the scope of this paper (see Haan et al., 2006, for more details).

4.0 EXPERIMENTAL STUDY OF GENERAL PERFORMANCE

The AABL Wind and Gust Tunnel facility became operational in October of 2005. This section reports the results of testing the bypass-duct gust generator of this facility. These results include overall performance parameters, velocity profiles in the aerodynamic test section, time dependence of the gusts and static pressure distribution around the circuit. The atmospheric boundary layer mode and open-return mode of the tunnel were not tested for this project, and hence not reported here. Testing these modes is planned for the future.

4.1 Gust Generator Performance Parameters

Table 3 lists comparisons between predictions made for gust generator performance parameters and the values measured in the AABL Wind and Gust Tunnel. The changes being quantified are differences in test section velocity, fan pressure drop and fan motor power when one switches from having the bypass duct open to having it closed. The design estimates were made before the facility was built using the original fan curve provided by the vendor. Once the facility was complete, it was found from in situ measurements that the vendor-provided fan curve predicted performance somewhat below the as-built performance of the system. In situ testing found that the fan flow rate was approximately 20% greater than that predicted by the vendor's fan curve. A fan curve adjusted for this in situ performance was used to identify the measured value of K_L^{BD}. The measured velocity change in the test section was used to estimate K_L^{BD} as given in Table 2.

Overall, the design estimates compared very well with measurements. The increased gust magnitude is primarily due to the lower than expected bypass duct loss coefficient, K_L^{BD}. The small change in the pressure drop across the fan will minimize the unsteady loading on the fan and will minimize the pressure fluctuations due to the actuation of the dampers.

4.2 Test Section Velocity

The maximum velocity in the Aero test section was measured to be 53 m/s (188 mph). During the design process, the uniformity of the velocity profile in the test section was a priority. The goal was to produce a uniform flow both with and without gust generation. Mean velocity and turbulence intensity profiles were measured in the AABL tunnel.

Velocity profiles were measured using an A.A. Labs constant temperature anemometer and a straight, hot wire probe. Figure 4 shows the horizontal profile of mean velocity and turbulence intensity in the test section with the bypass ducts open and closed. The velocity across the test section is within 1.5% of the centerline velocity and the turbulence intensity is less then 0.15%. This same degree of uniformity and low turbulence is evident in the vertical velocity profiles (not shown). Clearly, the tunnel's flowconditioning devices (three screens and a honeycomb) is adequate to generate gusts while maintaining very uniform flow. The profiles show very little difference in turbulence intensity whether the bypass duct was open or closed. This shows that the bypass duct system is not generating unwanted turbulence in the test section.

4.3 Static Pressure Distribution

The design static pressures, as given in Table 1, are compared with those measured at each section of the wind tunnel (Figure 3). The comparison was found to be reasonable. The total wind tunnel loss coefficients compare very well between design and estimated values (Table 2).

4.4 Fan Section Velocity Profiles

The nature of non-uniformities ingested by the fan was quantified using an 18-hole pressure probe (a Dantec model PS18 Omniprobe) that could measure three components of velocity just upstream of the fan. Since the fan rotates through velocity asymmetries, it is subject to unsteady loading. The purpose of this test was to quantify any asymmetries induced by the bypass duct. The largest asymmetry going from a bypass open to closed configuration was approximately 17%. All other bypass-induced asymmetries were less than this—many were significantly less than this. It was assumed that if the flow asymmetries generated by the bypass duct were less than that generated by a typical ABL profile (30%-60%) then the bypass performance would be deemed acceptable. The level of inflow asymmetry of the system was therefore considered acceptable.

4.5 Time Dependence of Gusts

A hot wire anemometer was used to quantify the time scales of the gusts in the main test section. Figure 5 shows a velocity time series during a ramp up gust event. In this event the damper valves in the bypass duct go from fully open to fully closed causing an increase in the test section velocity of approximately 27%. The velocity magnitude reaches 97% of the increased steady-state (or gust) value in 2.2 seconds. In this case, the initial velocity was about 20 m/s and the final steady-state value was 25.4 m/s. This results in a velocity acceleration value of about 2.45 m/s^2. It was observed that this 2.2 second time interval decreases approximately linearly when the initial wind tunnel velocity is increased. Testing the gusts with initial wind tunnel velocities from 10 m/s to 25 m/s reduced the time interval for velocity change from 5.5 sec. to about 1 sec. The lower time interval will result in a velocity acceleration of 5.4 m/s^2. If the velocity is increased further it is possible to achieve the higher velocity acceleration limit of 10 m/s^2 that was set for the design.

5.0 SUMMARY

A unique wind tunnel with a active gust generation mechanism has been developed. The tunnel's performance has been at par with the design. The maximum test section velocity in the tunnel (53 m/s, 118 mph) will exceed the design estimate of 107 mph because the fan's performance was found to be slightly better than that initially specified by the vendor. The velocity in the Aero test section was found to be very uniform with turbulence less than 0.15%. A wide range of non-stationary flow structures can be simulated in the wind tunnel using a bypass duct with flow diverted through the use of computer-controlled vanes. The current design allows for gusts between 25% and 30% of the mean flow velocity with time and velocity acceleration scales comparable to a wide range of full scale thunderstorm and hurricane gust events.

6.0 ACKNOWLEDGMENTS

The authors are grateful for the support of the Department of Aerospace Engineering, T.A. Wilson and Grace Miller Endowment and the College of Engineering at Iowa State University. The support of the U.S. National Science Foundation (Grant # CMS-0201510) is also gratefully acknowledged. The authors would like to thank Professor Cesar Farell for his help designing the facility. In addition, the authors thank technician Bill Rickard and undergraduate students Joshua Clemens, John Stronck and Kevin

Houstman in the Aerospace Engineering department for their work on building and testing components of the system.

7.0 REFERENCES

Bearman, P.W., Morel, T. (1983), "Effect of free stream turbulence on the flow around bluff bodies," *Progress in Aerospace Sci.*, v. 20, 97-123.

Bienkiewicz, B., Cermak, J.E., Peterka, J.A., Scanlan, R.H. (1983), "Active Modeling of Large-Scale Turbulence." *Journal of Wind Engineering and Industrial Aerodynamics*, v. 13, 465-475.

Cermak, J.E. (1971), "Laboratory simulation of the atmospheric boundary layer," *AIAA Journal*, 9 (9), 1746-1754.

Cermak, J.E., Leighton, S.C., Leffler, R.D. (1995), "Wind-tunnel modeling of the atmospheric surface layer." *Journal of Wind Engineering and Industrial Aerodynamics*, v. 54/55, 505-513.

Chen, L., Letchford, C. (2005), "Simulation of Extreme Winds from Thunderstorm Downbursts," *Proc. 10th America's Conference on Wind Engineering*, Baton Rouge, Louisiana.

Cook, N.J. (1973), "On Simulating the Lower Third of the Urban Adiabatic Boundary Layer in a Wind Tunnel." *Atmospheric Environment*, v. 7, 691-705.

Davenport, A.G. (1966), "The treatment of wind loading on tall buildings," *Proc. Symposium On Tall Buildings*.

Farell, C., Iyengar, A.K.S. (1999), "Experiments on the wind tunnel simulation of atmospheric boundary layers," *Journal of Wind Engineering and Industrial Aerodynamics*, v. 79, 11-35.

Gartshore, I.S. (1973), "*The effects of free stream turbulence on the drag of rectangular two-dimensional prisms*," Boundary Layer Wind Tunnel Laboratory 4-73, University of Western Ontario.

Haan, Jr., F.L., P.P. Sarkar, N. Spencer-Berger, "Development of an Active Gust Generation Mechanism on a Wind Tunnel for Wind Engineering and Industrial Aerodynamics Applications," in review for publication in *Wind and Structures*.

Hillier, R., Cherry, R.J. (1981), "The effect of stream turbulence on separation bubbles," *Journal of Wind Engineering and Industrial Aerodynamics*, v. 8, 49-58.

Kareem, A., Cermak, J.E. (1979), "Wind-tunnel simulation of wind structure interactions," *ISA Transactions*, v. 18, n. 4, 23-41.

Kiya, M., Sasaki, K. (1985), "Structure of large-scale vortices and unsteady reverse flow in the reattaching zone of turbulent separation bubble," *Journal of Fluid Mechanics*, v. 154, 463-491.

Kobayashi, H., Hatanaka, A., Ueda, T. (1994), "Active simulation of time histories of strong wind gust in a wind tunnel." *Journal of Wind Engineering and Industrial Aerodynamics* v. 53, 315-330.

Melbourne, W.H. (1979), "Turbulence effects on maximum surface pressure – A mechanism and possibility of reduction," *Wind Engineering, Proc. of Fifth International Conference.* Pergamon Press.

Nakamura, Y., Ohya, Y. (1984), "The effects of turbulence on the mean flow past two-dimensional rectangular cylinders." *Journal of Fluid Mechanics*, v. 149, 255-273.

Saric, W.S. (1992), "The ASU Transition Research Facility," AIAA 17th Aerospace Ground Testing Conference, AIAA-92-3910.

Saathoff, P.J., Melbourne, W.H. (1997), "Effects of free-stream turbulence on surface pressure fluctuations in a separation bubble," *Journal of Fluid Mechanics*, v. 337, 1-24.

Saric, W.S. (1992), "The ASU Transition Research Facility," *AIAA 17th Aerospace*

Ground Testing Conference, AIAA-92-3910.

Schroeder, J.L., Smith, D.A. (1999), "Hurricane Bonnie wind flow characteristics as determined from WEMITE." *Wind Engineering into the 21st Century, Proc. of Tenth International Conference on Wind Engineering*, 329-335.

Tieleman, H.W., Akins, R.E. (1990), "Effects of incident turbulence on pressure distributions on rectangular prisms," *Journal of Wind Engineering and Industrial Aerodynamics*, v. 36, 579-588.

Wang, L., Kareem, A. (2005), "Modeling and Simulation of Transient Winds in Downbursts/Hurricanes," *Proc. 10th America's Conference on Wind Engineering*, Baton Rouge, Louisiana.

Wu, F., Sarkar, P.P., Mehta, K.C. (2001a), "Full-scale study of conical vortices and roof corner pressures," *Wind & Structures*, v. 4, n. 2,131-146.

Wu, F., Sarkar, P.P., Mehta, K.C., Zhao, Z. (2001b), "Influence of incident wind turbulence on pressure fluctuations near flat-roof corners," *Journal of Wind Engineering and Industrial Aerodynamics*, v. 89, 403-420.

Table 1. Design static pressure and estimated loss coefficients for tests in aerodynamic test section in closed-return mode of operation (with gust generator slots closed)

Exit Section of Components Listed	**Area m^2 (ft^2)**	**Length m (ft)**	**Local Design Velocity m/s**	**Design Static Pressure N/m^2**	**Estimated Loss Coefficient $K_L^{WTclean}$**
ABL Test Section	5.39 (58)	10.36 (34.00)	39.6	249.9	0.044
First Diffuser	5.95 (64)	2.29 (7.50)	35.9	342.6	0.055
First Corner	5.95 (64)	2.88 (9.45)	35.9	232.6	0.080
Duct between First and Second Corners	5.95 (64)	4.88 (16.00)	35.9	215.2	0.0126
Second Corner	5.95 (64)	2.88 (9.45)	35.9	105.2	0.080
First Transition	6.36 (68.4)	1.83 (6.00)	33.6	194.5	0.0053
First By-Pass Connector	6.36 (68.4)	1.52 (5.00)	33.6	189.0	0.0040
Fan/Motor/Nacelle	5.91 (63.6)	3.51 (11.50)	36.1	956.4	
Second By-Pass Connector	5.91 (63.6)	1.52 (5.00)	36.1	950.9	0.0040
Second Transition and Second Diffuser	20.7 (222.75)	19.1 (62.5)	10.3	1521.2	0.1080
Heat Exchanger	20.7 (222.75)	0.30 (1.0)	10.3	1431.8	0.0075
Third Corner	20.7 (222.75)	5.47 (17.95)	10.3	1421.5	0.0040
Third Diffuser and Duct	21.32 (229.5)	2.21 (7.25)	10.0	1419.6	0.00407
Fourth Corner	21.32 (229.5)	5.62 (18.45)	10.0	1410.0	0.0070
Plenum	21.32 (229.5)	2.90 (9.50)	10.0	1248.3	0.1176
Contraction	4.46 (48)	5.94 (19.50)	47.9	-87.1	0.0150
Aero Test Section	4.67 (50.3)	61.10 (20.00)	45.7	0.00	0.026
TOTAL		79.3 (260.1)			0.64

Table 2. Loss coefficients for wind tunnel main circuit (closed-return mode) and bypass duct circuit in different configurations.

	Description	Design Estimate	Measured
$K_L^{WT_{clean}}$	Slots covered	0.64	0.67
$K_L^{WT_{closed}}$	Slots uncovered, bypass duct closed	0.71	0.72
$K_L^{WT_{open}}$	Slots uncovered, bypass duct open	1.07	1.11
K_L^{BD}	Bypass duct loss coefficient	15.2	13.9

Table 3. Gust generator performance when conducting a change from a bypass-duct open condition to a bypass-duct closed condition.

	Velocity Change	Fan Pressure Change	Fan Power Change
Design Estimate	21%	4%	1%
Measured	27%	-2%	7%

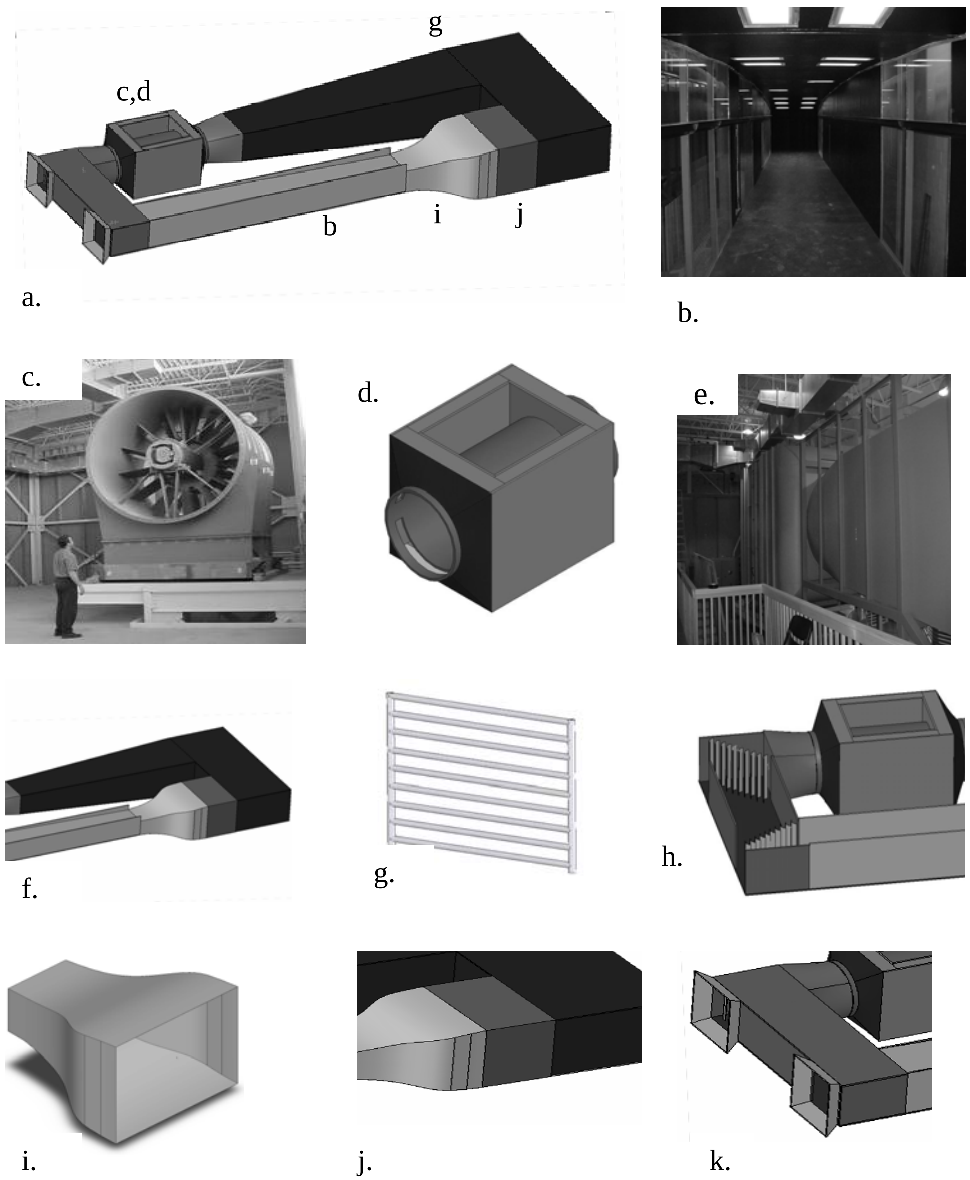

Figure 1. a. Layout of the AABL Wind and Gust Tunnel, b. Test sections as seen from downstream end, c. Fan section, d. By-pass gust generator-schematic, e. By-pass gust generator, f. Diffusers-schematic, g. Heat exchanger-schematic, h. Corner-schematic (first and second corners), i. Contraction-schematic, j. Plenum-schematic, k. Inlet and outlet for open–mode operation-schematic

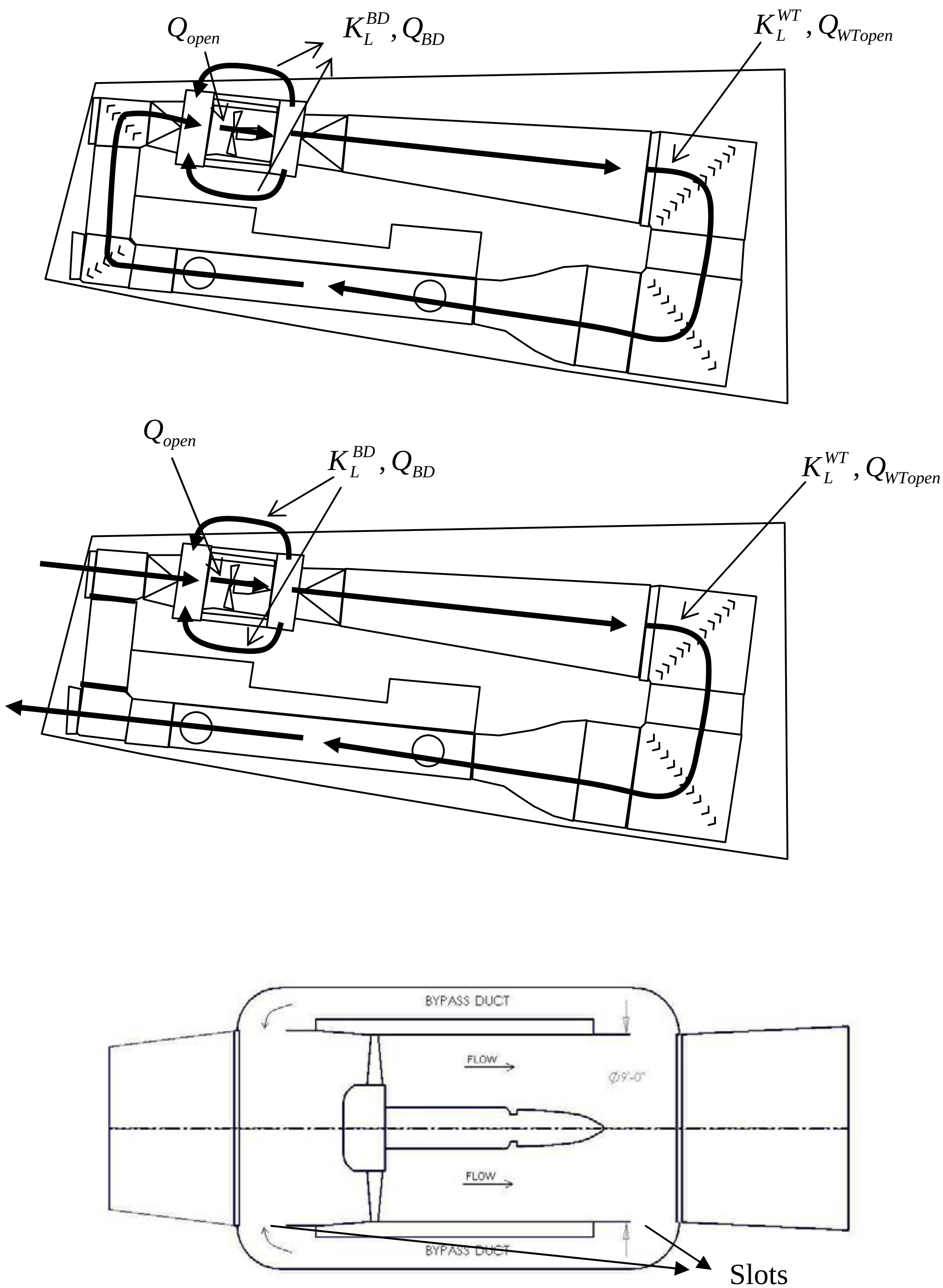

Figure 2. Diagrams showing the wind tunnel's main circuit and bypass duct in both closed and open circuit modes and the bypass duct surrounding the portion of the main duct containing the fan. The slots that allow flow through the bypass duct are covered when the gusting mode is not used.. K_L^{WT} and K_L^{BD} represent the loss coefficients through the wind tunnel test section and bypass duct circuits, respectively. Q_{BD}, Q_{WTopen} and Q_{open} are the flow rates through the bypass duct, the test section and the fan section, respectively.

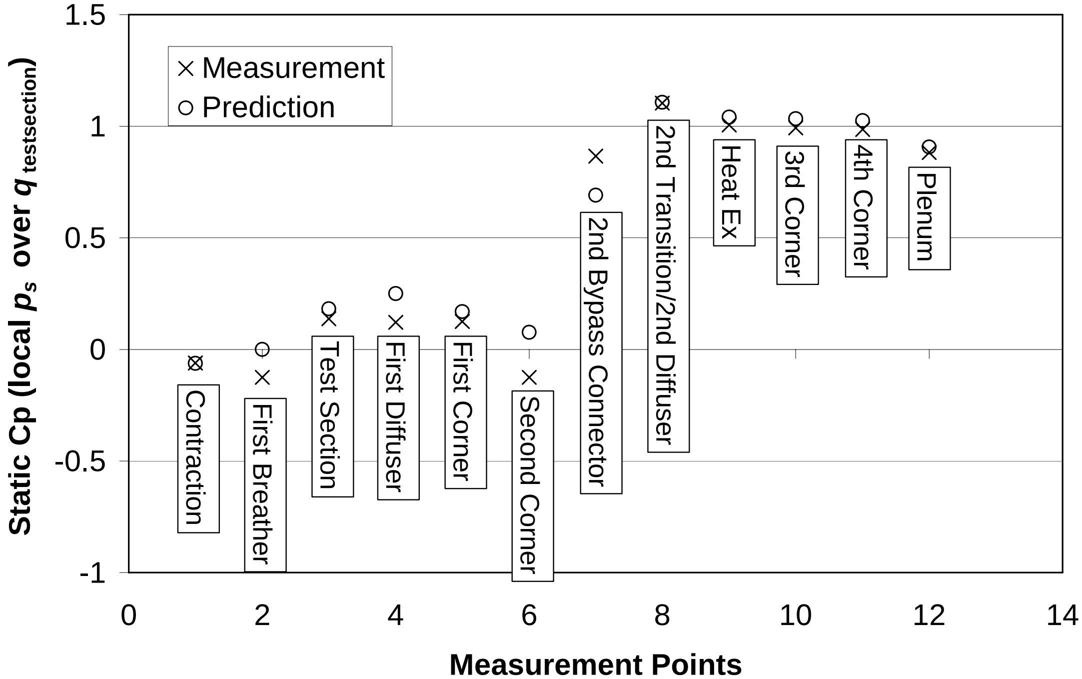

Figure 3. Comparison of static pressures at different sections of the ISU-AABL Wind and Gust Tunnel between design and measured values (closed-circuit mode, slots covered).

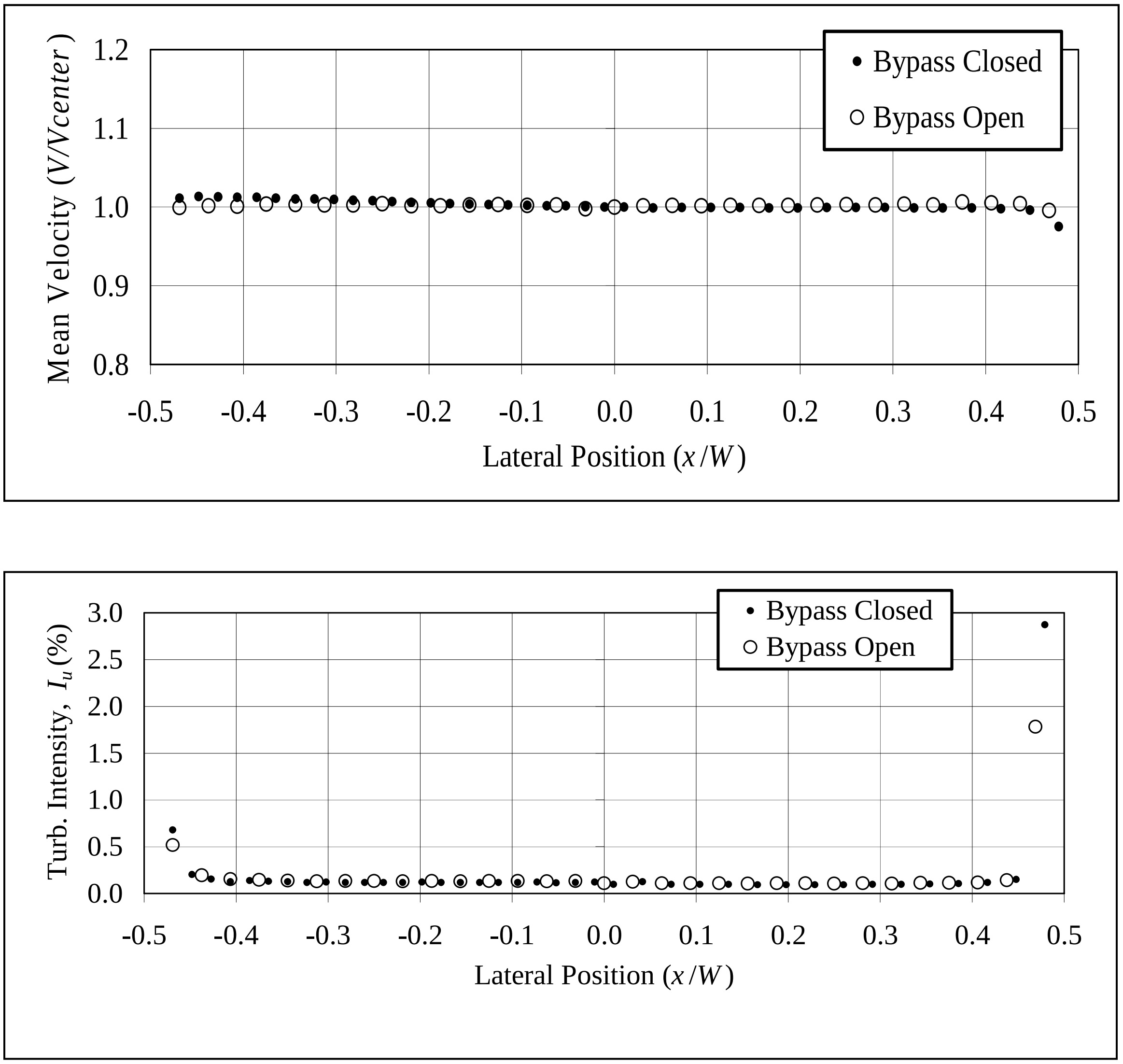

Figure 4. Horizontal profiles of mean test section velocity and turbulence intensity for bypass open and bypass closed cases.

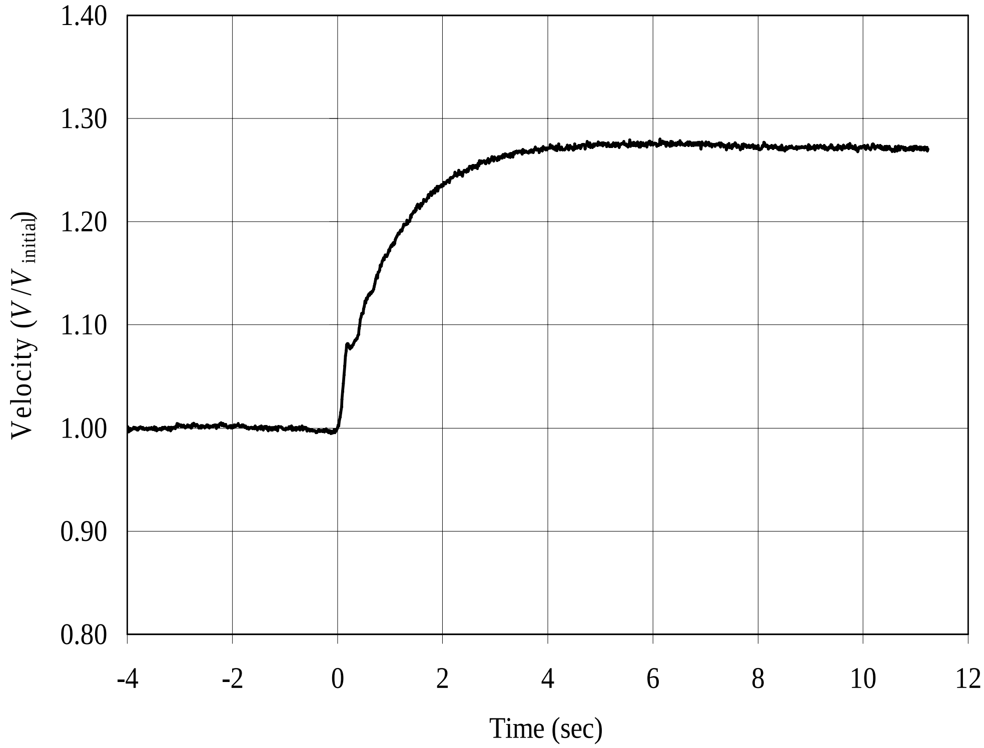

Figure 5. Time series of test section velocity during a ramp-up gusting event. 97% of the higher-speed velocity is attained within 2.2 seconds.